

# Characteristics of SnO<sub>2</sub>:F Thin Films Deposited by Ultrasonic Spray Pyrolysis: Effect of Water Content in Solution and Substrate Temperature

Mario Alberto Sánchez-García<sup>1</sup>, Arturo Maldonado<sup>2</sup>, Luis Castañeda<sup>3</sup>, Rutilo Silva-González<sup>3</sup>,  
María de la Luz Olvera<sup>2\*</sup>

<sup>1</sup>Institute of Physics, National Autonomous University of Mexico (UNAM), Apartado Postal 20-364, México D.F. 04510, Mexico; <sup>2</sup>Electrical Engineering Department, Solid State Electronics Section, Apartado 14740, México D.F. 07360, Mexico; <sup>3</sup>Institute of Physics, Autonomous Meritorious University of Puebla, Apartado Postal J-48, Puebla 72570, Mexico.  
Email: \*molvera@cinvestav.mx

Received July 9<sup>th</sup>, 2012; revised August 10<sup>th</sup>, 2012; accepted September 11<sup>th</sup>, 2012

## ABSTRACT

Fluorine doped tin oxide, SnO<sub>2</sub>:F, thin films were deposited by ultrasonic chemical spray starting from tin chloride and hydrofluoric acid. The physical characteristics of the films as a function of both water content in the starting solution and substrate temperature were studied. The film structure was polycrystalline in all cases, showing that the intensity of (200) peak increased with the water content in the starting solution. The electrical resistivity decreased with the water content, reaching a minimum value, in the order of  $8 \times 10^{-4} \Omega\text{cm}$ , for films deposited at 450°C from a starting solution with a water content of 10 ml per 100 ml of solution; further increase in water content increased the corresponding resistivity. Optical transmittances of SnO<sub>2</sub>:F films were high, in the order of 75%, and the band gap values oscillated around 3.9 eV. SEM analysis showed uniform surface morphologies with different geometries depending on the deposition conditions. Composition analysis showed a stoichiometric compound with a [Sn/O] ratio around 1:2 in all samples. The presence of F into the SnO<sub>2</sub> lattice was detected, within 2 at % respect to Sn.

**Keywords:** Tin Oxide; Ultrasonic Spray Pyrolysis; Transparent Conducting Oxides; TCO

## 1. Introduction

Semiconductor oxide thin films are materials with numerous applications in electronic and optoelectronic devices as well as some other applications such as protective coatings, heat mirrors, and catalysis [1-3]. In the context of world energy demand, particularly energy conversion, transparent conductive oxides (TCOs) based on semiconductor oxides, play a crucial role in the development of new-fashioned thin film solar cells [4]. As a matter of fact, in the organic solar cells, such as in dye-sensitized nanocrystalline TiO<sub>2</sub> solar cells (DSSCs), TCOs are used in tandem structures developed on ordinary glass and flexible substrates [5].

In this respect, TCOs for DSSCs manufacturing should present a good chemical stability due to the possible chemical reactions occurring in the manufacturing process, as in the annealing steps, and also the chemical interactions promoted by electrolytes in the line of duty, that define the lifetime of the device. In our developed work on organic thin film solar cells, we have noticed

that tin oxide electrodes offer the chemical stability required for device processing, contrary to results obtained from indium oxide films that, despite the higher electrical conductivity, is presented a degradation to metallic indium during the process, which in turn affects adversely the performance of the device.

The manufacturing of thin film devices based on non-sophisticated techniques, with a competitive performance has encouraged many researchers in the challenge of reaching higher efficiencies through the improvement of the material properties. Chemical deposition techniques provide a simple and economical way of processing good quality films demanded in the manufacturing of different devices. Some of the relevant chemical techniques for the deposition of quality films are sol-gel [6], homogeneous precipitation [7], chemical vapor deposition [8], and chemical spray techniques [9], among others. Results about deposition of quality SnO<sub>2</sub> films by chemical spray technique either in pneumatic or ultrasonic atomization process have been continuously reported [10,11]. In the pneumatic process, the deposition is developed at atmospheric pressure and the system is very simple; whereas in the

\*Corresponding author.

ultrasonic, it is necessary a closed reaction chamber, as a diluted fog instead of a jet of droplets is now directed on the hot substrate. In this deposition technique any slight disturbance generated by the exhaust system can modify the fog pattern, causing a non uniform growth, and hence, films with a like-rainbow finish are obtained. Nevertheless, according to our experience an advantage of the ultrasonic route is the significantly saving of reactants during the processing films.

As a consequence of the economic adaptation of the atomization equipment, the number of reports on SnO<sub>2</sub> thin films by ultrasonic spray is increasing now, and a better understanding of the process involved is being reached. Studies on the effect of post annealing treatments [12], substrate temperature [13], texture [14], microstructure [15], and doping [16] have been published. E. Elangovan, *et al.* [11] reported SnO<sub>2</sub>:F thin films with a resistivity in the order of  $2 \times 10^{-4} \Omega\text{cm}$ , starting from stannous chloride (SnCl<sub>2</sub>) and ammonium fluoride (NH<sub>4</sub>F). Also, the role of solution preparation in the deposition of tin oxide films by chemical spray technique has been raised [17]. Tin oxide thin films deposited by ultrasonic spray pyrolysis are usually reported starting from SnCl<sub>2</sub> and ethanol. In our case due to limitations of equipment, methanol has been adopted as the main solvent, since this can be atomized easily.

In this work, the effect of both water content in the starting solutions and substrate temperature on the physical characteristics of SnO<sub>2</sub> films, deposited by ultrasonic spray pyrolysis, starting from tin chloride and hydrofluoric acid, is reported.

## 2. Experimental

SnO<sub>2</sub>:F thin films were deposited by ultrasonic spray pyrolysis from a 0.2 M starting solution of tin chloride (SnCl<sub>4</sub>·5H<sub>2</sub>O), dissolved in a mix of water and methanol. The water content was varied in five different volumes, namely, 2.5, 5.0, 10.0, 20.0 and 30.0 ml for a total solution volume of 100 ml. Hydrofluoric acid at a fixed [F]/[Sn] ratio of 30 at % was used as F precursor. The selection of this ratio is based in previous experimental work, where we found that the optimum fluorine doping concentration oscillate between 20 and 40 at %.

SnO<sub>2</sub>:F samples were deposited on 2.5 cm × 5.0 cm clean glass substrates at five different substrate temperatures, namely, 375°C, 400°C, 425°C, and 450°C, at a fixed deposition time of 12 min. The cleaning process was as follows: 1) a five minutes ultrasonic bath in a trichloroethylene for degreasing the substrates; followed by 2) a five minutes bath in methyl alcohol; 3) a five minutes ultrasonic bath in acetone [CH<sub>3</sub>COCH<sub>3</sub>]; and finally, 4) a drying process by a jet of gas nitrogen [N<sub>2</sub>].

The electrical sheet resistance of all as-deposited samples was measured by the four point probe technique by using a Veeco equipment, with the appropriate geometric correction,  $\pi/\ln 2 = 4.53$ . The structure of the as-deposited films was characterized by means of X-ray diffraction in a Pan-Analytical XPert Pro system, by using the  $\theta - 2\theta$  technique, based on the Cu-K $\alpha$  radiation ( $\lambda = 1.5405 \text{ \AA}$ ). Scanning electron micrographs were obtained from a Jeol JSM 5400 LV microscope. Chemical composition of all the SnO<sub>2</sub> films was determined by energy dispersive spectroscopy (EDS) with a detector MORAN (Quest) having a 136 eV resolution. The optical transmittance at normal incidence was measured with a double-beam UV-Vis Shimadzu spectrophotometer, in the UV-visible region (300 - 1000 nm) without glass substrate correction. The film thickness was estimated according to the Manificier's formula [18], and corroborated by direct measurements with a KLA Tencor P15 profilometer. The values estimated were around 600 nm.

## 3. Results and Discussion

### 3.1. Electrical Properties

Electrical resistivities for all as-grown SnO<sub>2</sub>:F films deposited were calculated from the mathematical product of the respective sheet resistances and thickness values. In **Table 1** are listed the results obtained. From these, it can be observed that an increase in the water content leads to a decreasing in the electrical resistivity, reaching a minimum magnitude in samples deposited at 450°C from a starting solution with  $\text{Vol}_{\text{H}_2\text{O}}/\text{Vol}_{\text{TOTAL}} = 10/100$ . Further increase in the substrate temperature increases the electrical resistance of the films. These results show that both substrate temperature and water content influence the growth kinetic and consequently the physical properties of the films. This behavior is associated with the variation of the F incorporation into the SnO<sub>2</sub> lattice as the solution conditions and deposition temperature are changed.

**Table 1. Electrical resistivity values of SnO<sub>2</sub>:F films deposited at different substrate temperatures, from starting solutions with different  $\text{Vol}_{\text{H}_2\text{O}}/\text{Vol}_{\text{TOTAL}}$  ratios.**

Deposition Temperature (°C)	2.5/100 $\times 10^{-4}$ ( $\Omega \cdot \text{cm}$ )	5/100 $\times 10^{-4}$ ( $\Omega \cdot \text{cm}$ )	10/100 $\times 10^{-4}$ ( $\Omega \cdot \text{cm}$ )	20/100 $\times 10^{-4}$ ( $\Omega \cdot \text{cm}$ )	30/100 $\times 10^{-4}$ ( $\Omega \cdot \text{cm}$ )
375	199	150	82	68	44
400	40	24	24	21	25
425	11	9	11	18	25
450	10	10	8	22	26

### 3.2. Structure

**Figure 1** shows the X ray diffraction spectra of SnO<sub>2</sub>:F thin films deposited at 450°C from starting solutions with different water contents, for  $2\theta$  values from 20° to 70°. All samples were polycrystalline, and the peaks fit well with the different reflections of the SnO<sub>2</sub> cubic rutile structure, ASTM standard card JCPDS No. 41-1445 [19]. All spectra show the (200) direction as preferred growth orientation, whereas the (110) and (310) directions increase with the water content in the starting solution. These results demonstrate that, as was expected, the preferred growth orientation is sensible to the water content in the starting solutions. Absence of the Sn<sub>3</sub>O<sub>4</sub> phase was also confirmed, as substrate temperatures higher than 400°C guarantee only SnO<sub>2</sub> formation. Additionally, no fluorine phases were detected despite the fact that a high [F/Zn] = 30 at % ratio in starting solution, was added. This result confirms the highly volatile character of fluorine compounds during the growth process, and consequently its low efficiency of incorporation into the SnO<sub>2</sub> lattice.

### 3.3. Morphology

**Figures 2** and **3** show the variation in the surface morphology of SnO<sub>2</sub>:F thin films deposited at 450°C as a function of the water content in the starting solution at different magnifications.

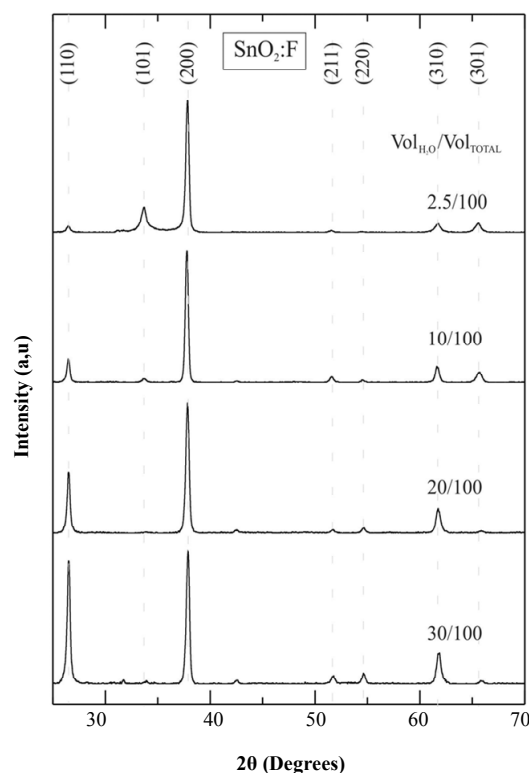


**Figure 1.** X-ray diffraction spectra of chemically sprayed SnO<sub>2</sub>:F thin films deposited at 450°C, from starting solutions with different water content.

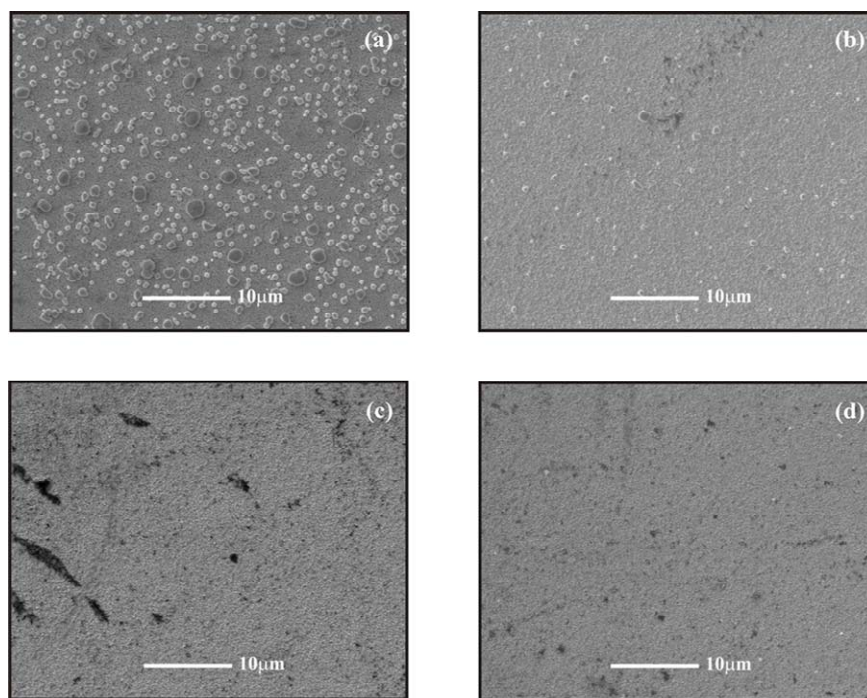


**Figure 2.** SEM micrographs at low magnification of SnO<sub>2</sub>:F thin films deposited at 450°C, from starting solutions with different water content. (a)  $\text{Vol}_{\text{H}_2\text{O}}/\text{Vol}_{\text{TOTAL}} = 2.5/100$ ; (b)  $\text{Vol}_{\text{H}_2\text{O}}/\text{Vol}_{\text{TOTAL}} = 10/100$ ; (c)  $\text{Vol}_{\text{H}_2\text{O}}/\text{Vol}_{\text{TOTAL}} = 20/100$ ; and (d)  $\text{Vol}_{\text{H}_2\text{O}}/\text{Vol}_{\text{TOTAL}} = 30/100$ .

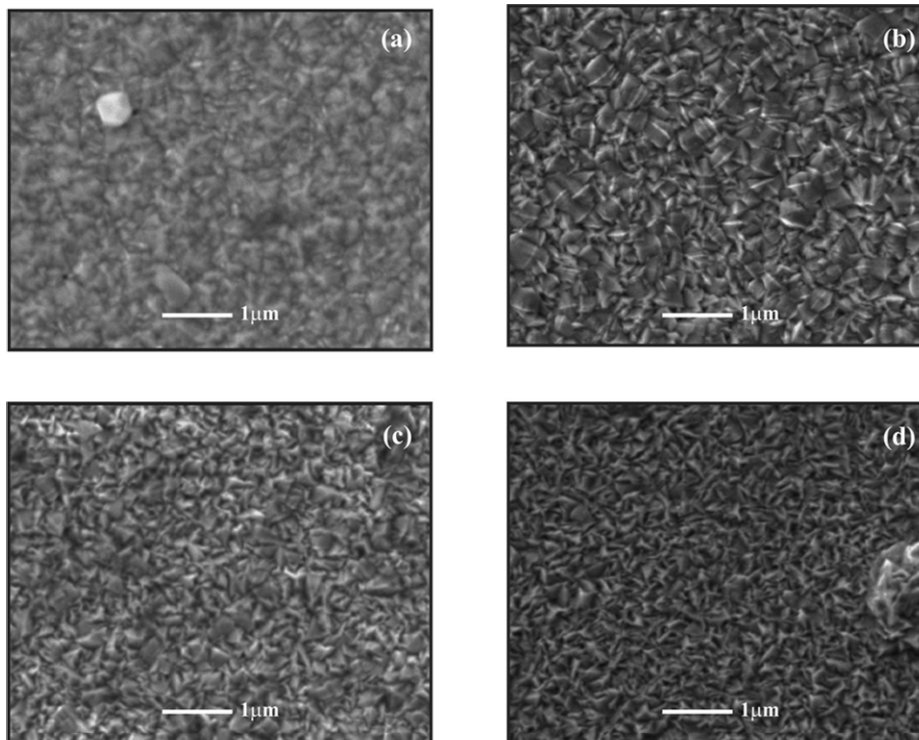


**Figure 3.** SEM micrographs at high magnification of SnO<sub>2</sub>:F thin films deposited at 450°C, from starting solutions with different water content. (a)  $\text{Vol}_{\text{H}_2\text{O}}/\text{Vol}_{\text{TOTAL}} = 2.5/100$ ; (b)  $\text{Vol}_{\text{H}_2\text{O}}/\text{Vol}_{\text{TOTAL}} = 10/100$ ; (c)  $\text{Vol}_{\text{H}_2\text{O}}/\text{Vol}_{\text{TOTAL}} = 20/100$ ; and (d)  $\text{Vol}_{\text{H}_2\text{O}}/\text{Vol}_{\text{TOTAL}} = 30/100$ .

In **Figure 2**, at low magnification, it can be seen that SnO<sub>2</sub> films deposited with the lowest water content ( $\text{Vol}_{\text{H}_2\text{O}}/\text{Vol}_{\text{TOTAL}} = 2.5/100$ , **Figure 2(a)**), a few secondary grains in the order of 1.5 μm are formed on the compact and uniform surface of the film; in the case of films deposited from a solution with a higher water content ( $\text{Vol}_{\text{H}_2\text{O}}/\text{Vol}_{\text{TOTAL}} = 10/100$ , **Figure 2(b)**), the number of secondary particles decreases both in number and size, whereas for the highest water content ( $\text{Vol}_{\text{H}_2\text{O}}/\text{Vol}_{\text{TOTAL}} = 30/100$ , **Figure 2(d)**) no particles can be observed. From a higher zoom of the images shows that grains of films deposited from solutions with the lowest water content present irregular size and shape, then it can be considered that grain size is ranging from 100 to 200 nm (**Figure 3(a)**). The surface of films deposited with a higher water content ( $\text{Vol}_{\text{H}_2\text{O}}/\text{Vol}_{\text{TOTAL}} = 10/100$ ) show an increase in the size, higher than 200 nm, and the geometry of the grains resembles a cylinder-shaped form (**Figure 3(b)**). The films deposited with a water content of 20/100 show a surface covered by triangular pyramids with irregular size, in the order of 150 nm (**Figure 3(c)**). Finally, the films deposited with the highest water content, 30/100, shows well-defined triangular pyramids with small dimensions compared with films deposited from a starting

solution with a water content of 20/100 (**Figure 3(d)**).

### 3.4. Optical Properties

**Figure 4** shows the optical transmittance spectrum of a SnO<sub>2</sub>:F thin film deposited from a starting solution containing the highest water content, 30/100, measured in the wavelength range from 300 to 1000 nm, taking the air as reference. All SnO<sub>2</sub>:F thin films were highly transparent in the visible range, with an optical transmittance in the order of 80% at the middle of the visible range (550 nm). The optical band-gap values,  $E_G$ , were determined according to Roth and Webb procedure [20], for heavily doped semiconductors, and from the absorption coefficient spectra  $\alpha(\lambda)$  computed from the Burguer-Lambert equation ( $I = I_0 \exp(-ad)$ ), where  $\alpha(\lambda)$  is the absorption coefficient, and  $d$  the film thickness [21]. A typical band gap calculation is reported in the inset in **Figure 4**, corresponding to the SnO<sub>2</sub>:F sample deposited from the starting solution with the highest water content, namely,  $\text{Vol}_{\text{H}_2\text{O}}/\text{Vol}_{\text{TOTAL}} = 30/100$ .

In general,  $E_G$  values were high, around 3.9 eV, irrespective of both water content in the starting solution and deposition temperature. This band gap increasing can be interpreted according to the Moss Burstein effect, which states that the increase in the free carrier concentration,

due to the high doping level, fills empty states belonging to conduction band, increasing the energy magnitude required for the valence band to conduction band transitions.

### 3.5. Chemical Composition

Compositional analysis of the elements present in the

films was performed on selected samples. **Figure 5** shows the EDS measurement of a SnO<sub>2</sub>:F thin film deposited at 450°C, from a Vol<sub>H<sub>2</sub>O</sub>/Vol<sub>TOTAL</sub> = 30/100 starting solution. Films are almost stoichiometric, with a Sn:O ratio of 1:2, found in all the films. However, the non-intentional incorporation of undesirable elements was also confirmed by EDS analysis, as Ca, Si, K, Mg were detected in all the samples.

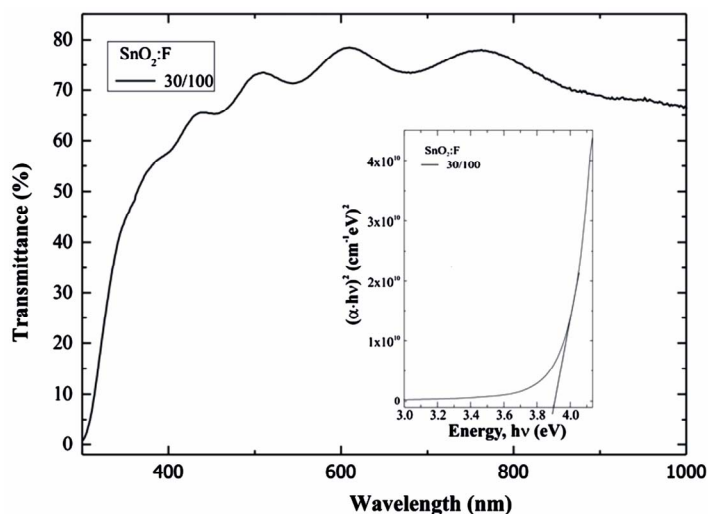


Figure 4. Optical transmittance SnO<sub>2</sub>:F thin films deposited at 450°C, from a Vol<sub>H<sub>2</sub>O</sub>/Vol<sub>TOTAL</sub> = 30/100 starting solution.

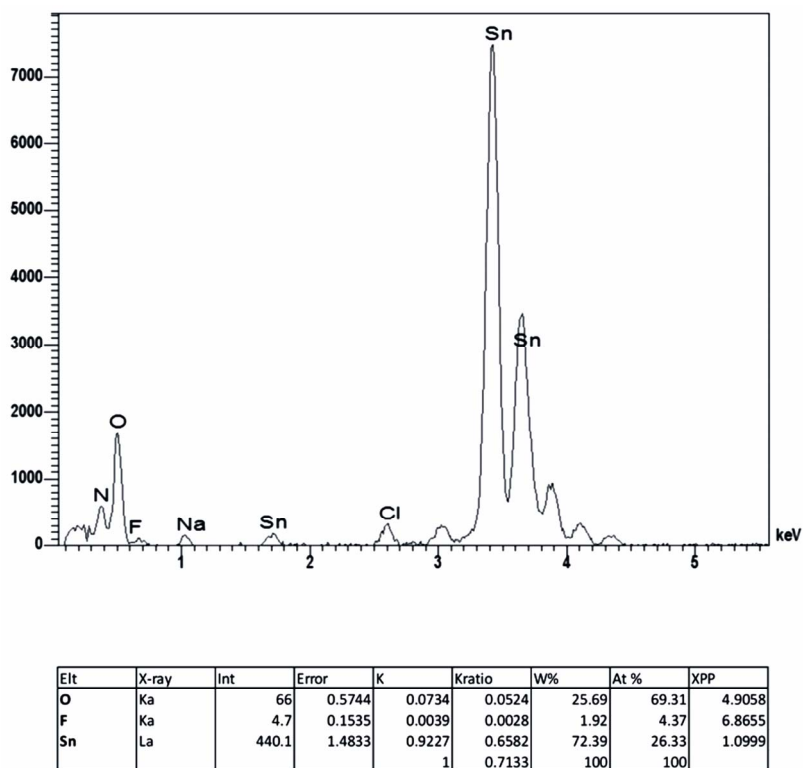


Figure 5. EDS measurements of SnO<sub>2</sub>:F thin films deposited at 450°C, from a Vol<sub>H<sub>2</sub>O</sub>/Vol<sub>TOTAL</sub> = 30/100 starting solution.



These elements come from the glass substrate due to exo-diffusion of impurities during the growth process, and are responsible of the increase in the electrical resistivity of the films. It is worthy of mention that nitrogen element was also detected into the lattice, although in a small quantity as compared with alkaline elements. It is hard to assume that nitrogen can dope the SnO<sub>2</sub> films effectively due to the fact that a low electrical resistivity was obtained. In this case a more careful study has to be done in order to figure out the specific sites where nitrogen is hosted. Fluorine was detected into the films and a variation ranging from 4 to 4.5 at % was measured. This value of fluorine atomic content into the SnO<sub>2</sub> lattice is consistent with other reported [22], however, there still remain the question about specific sites where F is incorporated, as clustering of fluorine or grain boundary segregation can occur.

#### 4. Conclusion

The characteristics of SnO<sub>2</sub>:F thin films deposited by ultrasonic spray pyrolysis (USP) as a function of both water content in starting solution and substrate temperature were studied. The minimum electrical resistivity and maximum optical transmittance in the UV-visible achieved for SnO<sub>2</sub>:F thin films were around  $8 \times 10^{-4}$  Ωcm and 75%, respectively. According to the results obtained, SnO<sub>2</sub>:F thin films deposited by USP can find application as transparent electrodes in organic thin film solar cells due to both the low resistivity measured and the high chemical stability presented.

#### 5. Acknowledgements

The technical assistance of M. A. Luna-Arias, J. E. Romero-Ibarra, A. Tavira-Fuentes, and A. Palafox is thanked. This work was partially supported by CONACyT under contract Number 166601.

#### REFERENCES

- [1] C. G. Granqvist, "Transparent Conductors as Solar Energy Materials: A Panoramic Review," *Solar Energy Materials & Solar Cells*, Vol. 91, No. 17, 2007, pp. 1529-1598. [doi:10.1016/j.solmat.2007.04.031](https://doi.org/10.1016/j.solmat.2007.04.031)
- [2] G. J. Exarhos and X.-D. Zhou, "Discovery-Based Design of Transparent Conducting Oxide Films," *Thin Solid Films*, Vol. 515, No. 18, 2007, pp. 7025-7052. [doi:10.1016/j.tsf.2007.03.014](https://doi.org/10.1016/j.tsf.2007.03.014)
- [3] S. Malato, P. Fernández-Ibáñez, M. I. Maldonado, J. Blanco and W. Gernjak, "Decontamination and Disinfection of Water by Solar Photocatalysis: Recent Overview and Trends," *Catalysis Today*, Vol. 147, No. 1, 2009, pp. 1-59. [doi:10.1016/j.cattod.2009.06.018](https://doi.org/10.1016/j.cattod.2009.06.018)
- [4] B. Li, L. D. Wang, B. N. Kang, P. Wang and Y. Qiu, "Review of Recent Progress in Solid-State Dye-Sensitized Solar Cells," *Solar Energy Materials & Solar Cells*, Vol. 90, No. 5, 2006, pp. 549-573. [doi:10.1016/j.solmat.2005.04.039](https://doi.org/10.1016/j.solmat.2005.04.039)
- [5] F. C. Krebs, "Fabrication and Processing of Polymer Solar Cells: A Review of Printing and Coating Techniques," *Solar Energy Materials & Solar Cells*, Vol. 93, 2009, pp. 394-412. [doi:10.1016/j.solmat.2008.10.004](https://doi.org/10.1016/j.solmat.2008.10.004)
- [6] G. Frenzer and W. F. Maier, "Amorphous Porous Mixed Oxides: Sol-Gel Ways to a Highly Versatile Class of Materials and Catalysts Annu," *Materials Research*, Vol. 36, 2006, pp. 281-331. [doi:10.1146/annurev.matsci.36.032905.092408](https://doi.org/10.1146/annurev.matsci.36.032905.092408)
- [7] G. Oskam, "Metal Oxide Nanoparticles: Synthesis, Characterization and Application," *Journal of Sol-Gel Science and Technology*, Vol. 37, No. 3, 2006, pp. 161-164. [doi:10.1007/s10971-005-6621-2](https://doi.org/10.1007/s10971-005-6621-2)
- [8] M. O. Nwodo, S. C. Ezugwu, F. I. Ezema, P. U. Asogwa and R. U. Osuji, "Chemical Bath Deposition and Characterization of PVD Capped Tin Oxide Thin Films," *Journal of Optoelectronics and Biomedical Materials*, Vol. 2, No. 4, 2010, pp. 267-272.
- [9] P. S. Patil, "Review Versatility of Chemical Spray Pyrolysis Technique," *Materials Chemistry and Physics*, Vol. 59, No. 3, 1999, pp. 185-198. [doi:10.1016/S0254-0584\(99\)00049-8](https://doi.org/10.1016/S0254-0584(99)00049-8)
- [10] A. A. Yadav, E. U. Masumdar, A. V. Moholkar, M. Neumann-Spallart, K. Y. Rajpure and C. H. Bhosale, "Electrical, Structural and Optical Properties of SnO<sub>2</sub>:F Thin Films: Effect of the Substrate Temperature," *Journal of Alloys and Compounds*, Vol. 488, No. 1, 2009, pp. 350-355. [doi:10.1016/j.jallcom.2009.08.130](https://doi.org/10.1016/j.jallcom.2009.08.130)
- [11] E. Elangovan, K. Ramamurthi, "Studies on Micro-Structural and Electrical Properties of Spray-Deposited Fluorine-Doped Tin Oxide Thin Films from Low-Cost Precursor," *Thin Solid Films*, Vol. 476, No. 2, 2005, pp. 231-236. [doi:10.1016/j.tsf.2004.09.022](https://doi.org/10.1016/j.tsf.2004.09.022)
- [12] K. B. Sundaram and G. K. Bhagavat, "High-Temperature Annealing Effects on Tin Oxide Films," *Journal of Physics D: Applied Physics*, Vol. 16, No. 1, 1983, pp. 69-76. [doi:10.1088/0022-3727/16/1/011](https://doi.org/10.1088/0022-3727/16/1/011)
- [13] C.-C. Lin, M.-C. Chiang and Y.-W. Chen, "Temperature Dependence of Fluorine-Doped Tin Oxide Films Produced by Ultrasonic Spray Pyrolysis," *Thin Solid Films*, Vol. 518, No. 4, 2009, pp. 1241-1244. [doi:10.1016/j.tsf.2009.05.064](https://doi.org/10.1016/j.tsf.2009.05.064)
- [14] C.-Y. Kim and D.-H. Riu, "Texture Control of Fluorine-Doped Tin Oxide Thin Film," *Thin Solid Films*, Vol. 519, No. 10, 2011, pp. 3081-3085. [doi:10.1016/j.tsf.2010.12.096](https://doi.org/10.1016/j.tsf.2010.12.096)
- [15] D. Jadsadapattarakul, C. Euvananont, C. Thanachayanont, J. Nukeawa and T. Sooknoi, "Tin Oxide Thin Films Deposited by Ultrasonic Spray Pyrolysis," *Ceramics International*, Vol. 34, No. 4, 2008, pp. 1051-1054. [doi:10.1016/j.ceramint.2007.09.096](https://doi.org/10.1016/j.ceramint.2007.09.096)
- [16] B. Zhang, Y. Tian, J. X. Zhang and W. Cai, "Structural, Optical, Electrical Properties and FTIR Studies of Fluorine Doped SnO<sub>2</sub> Films Deposited by Spray Pyrolysis," *Journal of Materials Science*, Vol. 46, No. 6, 2011, pp.

- 1884-1889. [doi:10.1007/s10853-010-5021-3](https://doi.org/10.1007/s10853-010-5021-3)
- [17] C. Luyo, I. Fábregas, L. Reyes, J. L. Solís, J. Rodríguez, W. Estrada and R. J. Candal, "SnO<sub>2</sub> Thin-Films Prepared by a Spray-Gel Pyrolysis: Influence of Sol Properties on Film Morphologies," *Thin Solid Films*, Vol. 516, No. 1, 2007, pp. 25-33. [doi:10.1016/j.tsf.2007.05.023](https://doi.org/10.1016/j.tsf.2007.05.023)
- [18] J. C. Manificier, J. Gasiot and J. P. Fillard, "A Simple Method for the Determination of the Optical Constants  $n$ ,  $h$  and the Thickness of a Weakly Absorbing Thin Film," *Journal of Physics E: Scientific Instruments*, Vol. 9, No. 11, 1976, p. 1002. [doi:10.1088/0022-3735/9/11/032](https://doi.org/10.1088/0022-3735/9/11/032)
- [19] Joint Committee on Powder Diffraction Standards (JCPDS), International Centre for Diffraction Data, 1997, Card No. 41-1445.
- [20] A. P. Roth and J. B. Webb, "Band-Gap Narrowing in Heavily Defect-Doped ZnO," *Physical Review B*, Vol. 25, No. 12, 1982, pp. 7836-7839.
- [21] F. R. Flory, "Thin Films for Optical Systems," Marcel Dekker, Inc., New York, 1995. pp. 285-287.
- [22] V. Bilgin, I. Akyuz, E. Ketenci, S. Kose and F. Atay, "Electrical, Structural and Surface Properties of Fluorine Doped Tin Oxide Films," *Applied Surface Science*, Vol. 256, No. 22, 2010, pp. 6586-6591. [doi:10.1016/j.apsusc.2010.04.052](https://doi.org/10.1016/j.apsusc.2010.04.052)